Role of the Oxyanion Binding Site and Subsites S1 and S2 in the Catalysis of Oligopeptidase B, a Novel Target for Antimicrobial Chemotherapy†

Tünde Juhász, Zoltán Szeltner, Veronika Renner, and László Polgár*

Institute of Enzymology, Biological Research Center, Hungarian Academy of Sciences, P.O. Box 7, Budapest H-1518, Hungary

Received December 7, 2001; Revised Manuscript Received January 30, 2002

ABSTRACT: Oligopeptidase B is a member of a novel serine peptidase family, found in Gram-negative bacteria and trypanosomes. The enzyme is involved in host cell invasion, and thus, it is an important target for drug design. Oligopeptidase B is specific for substrates with a pair of basic residues at positions P1 and P2. The sensitivity of substrates to high ionic strength suggests that the arginines interact with the carboxylate ions of the enzyme. On the basis of a three-dimensional model, two carboxyl dyads (Asp460 and Asp462 and Glu576 and Glu578) can be assigned as binding sites for arginines P1 and P2, respectively. The dyads are involved in several events: (i) substrate binding, (ii) substrate inhibition at high substrate concentrations (different inhibitory mechanisms were demonstrated with substrates bearing one and two arginine residues), (iii) enzyme activation at millimolar $CaCl_2$ concentrations with substrates having one arginine, and (iv) interaction of Ca^{2+} with the dyads which simplified the complex pH dependence curves. Titration with a product-like inhibitor revealed the pK_a of the carboxyl group that perturbed the pH−k_{cat}/K_m profiles. The OH group of Tyr452 is part of the oxyanion binding site, which stabilizes the transition state of the reaction. Its role studied with the Tyr452Phe variant indicates that (i) the catalytic contribution of the OH group depends on the substrate and (ii) the catalysis is, unusually, an entropy-driven process at physiological temperature. The NH group of the scissile peptide bond accounts for the deviation of the reaction from the Eyring plot above 25 °C, and for abolishing potential nonproductive binding.

A new class of serine peptidases (clan SC, family S9) has recently been identified and called the prolyl oligopeptidase family (*1*, *2*). The members of this family, such as the prototype prolyl oligopeptidase, dipeptidyl peptidase IV, acylaminoacyl peptidase, and oligopeptidase B, exhibit much larger molecular masses (∼80 kDa) with respect to the most extensively studied serine peptidases, chymotrypsin and subtilisin. The catalytic domain of the members of the prolyl oligopeptidase family, which is at the C-terminus of a single polypeptide chain, is structurally related to lipases of the α/β-hydrolase fold rather than to peptidases (*3*). This was confirmed by the determination of the three-dimensional structure of one family member, namely, prolyl oligopeptidase (*4*). The results have also shown that the N-terminal domain of the enzyme is an unusual β-propeller, which accounts for the oligopeptidase activity by excluding large peptides from the active site (*5*). The catalytic triad (Ser554, Asp641, and His680) is located at the interface of the two domains.

Oligopeptidase B (EC 3.4.21.83), previously called protease II, is homologous to prolyl oligopeptidase, indicating that the tertiary structures of the two enzymes are similar (*6*, *7*). Oligopeptidase B was first isolated from *Escherichia coli* cells with trypsin-like specificity, cleaving peptides at lysine and arginine residues (cf. ref *8*). The enzyme is also present in protozoan parasites, such as *Trypanosoma cruzi*, the causative agent of Chagas disease in humans (*9*), and the African trypanosomes of the *Trypanosoma brucei* group (*10*−*12*) that produce the diseases nagana and sleeping sickness in cattle and humans, respectively. The enzyme is implicated in host cell invasion by the parasite by generating an active Ca^{2+} agonist from a cytosolic precursor molecule (*13*−*15*). Antibodies to the recombinant oligopeptidase B inhibited both peptidase activity and Ca^{2+} signaling (*13*). Oligopeptidase B activity correlates with blood parasitemia level. Since the trypanosomes do not release oligopeptidase B in vitro, it was proposed that disrupted cells of *T. brucei* release the enzyme into circulation, where it exerts its detrimental effects (*16*).

Oligopeptidase B hydrolyzes much faster peptides with two adjacent basic residues than substrates with a single base (*17*−*19*). The k_{cat}/K_m for Z-Arg-Arg-Amc[1] is extremely high (63 μM^{-1} s^{-1}) at low ionic strength, and this preference for adjacent arginine residues indicates that oligopeptidase B may be a new type of processing enzyme (*19*).

The catalytic mechanism of oligopeptidases is similar to that of the trypsin and subtilisin type enzymes. Specifically, the serine OH group of the catalytic triad reacts with the

† This work was supported by OTKA T/11 (Grant T029056), the Human Frontier Science Program (RG0043/2000-M 102), Wellcome Collaborative Research Initiative Grant 055178/Z/97/Z/98/Z, and the British-Hungarian Science and Technology Program (GB 18/98).

* To whom correspondence should be addressed: Institute of Enzymology, BRC, Hungarian Academy of Sciences, P.O. Box 7, Budapest H-1518, Hungary. Fax: 36-1-466-5465. E-mail: polgar@hanga.enzim.hu.

[1] Abbreviations: DMF, dimethylformamide; EDTA, ethylenediaminetetraacetic acid; Mes, 2-(morpholino)ethanesulfonic acid; Cit, citrulline; Z, benzyloxycarbonyl; Bz, benzoyl; Amc, 7-(4-methylcoumaryl)amide; Nan, 4-nitroanilide; Nap, 2-naphthylamide; Et, OC_2H_5.

10.1021/bi016016z CCC: $22.00
Published on Web 00/00/0000 PAGE EST: 10.8

peptide carbonyl carbon atom of the substrate, and this process generates a tetrahedral intermediate that possesses a negatively charged oxygen atom. The transition state resembles this intermediate that decomposes to the acyl enzyme, which is, in turn, hydrolyzed by a water molecule. Both the formation and breakdown of the acyl enzyme are facilitated by the histidine residue as a general base/acid catalyst (*20*).

A distinct event in the catalysis of oligopeptidases concerns the stabilization of the negatively charged tetrahedral intermediate. The oxyanion binding site that provides two hydrogen bonds to the oxyanion achieves the stabilization. In the trypsin type enzymes, the hydrogen bonds are contributed by two main chain NH groups, while in subtilisin and its homologues, one of the hydrogen bonds originates from the side chain amide of an asparagine residue (*20*−*22*). In prolyl oligopeptidase, one of the hydrogen bonds is generated between the oxyanion and the main chain NH group of Asn555, while the other bond is formed with the Tyr473 OH group (*4*, *23*). In oligopeptidase B, Tyr452 corresponds to Tyr473 of prolyl oligopeptidase, which is obvious from the alignment of the amino acid sequences (*6*), and from the site-specific mutagenesis study reported here.

Because of the role of oligopeptidase B in several widespread tropical diseases, brought about by eukaryotic unicellular parasites, and in other infectious illnesses caused by Gram-negative bacteria, we have undertaken an investigation of the catalytic mechanism and substrate recognition properties of the enzyme, the knowledge of which is essential for effective drug design.

EXPERIMENTAL PROCEDURES

Enzymes. Oligopeptidase B was overexpressed in *E. coli* JM83 cells, purified, and assayed as described previously (*24*). The concentration of the enzyme was determined at 280 nm, using a molecular mass of 81 858 Da and an A_{280} of 1.83 for a concentration of 1.0 mg/mL (*24*).

The Tyr452Phe mutation was introduced with the two-step PCR procedure as described for the site-specific mutagenesis of prolyl oligopeptidase (*23*). In short, four oligonucleotides were synthesized. Those designed to the 5′- and 3′-ends of the gene contained *Eco*RI and *Sal*I restriction sites (underlined), respectively, while the mutagenic primers with the TTT codon for phenylalanine had a *Bam*HI site (underlined): to the 5′-end, 5′-CGGAATTCATCCCCGGTGAGTTTTGC-3′; to the 3′-end, 5′-ACGCGTCGACGAACGCGATCCGGGCTA-3′; sense primer, 5′-GTGTATGGCTTTGGATCCTACGGC-3′; and antisense primer, 5′-GCCGTAGGATCCAAAGCCATACAC-3′.

In the first step of PCR, two independent reactions were carried out, using the Vent polymerase and the pSK/OpB plasmid as a template digested with the *Eco*RI enzyme. To this mixture were added the 5′-primer and the antisense mutagenic primer for the first reaction. In the second reaction, the 3′-primer and the sense mutagenic primer were added, using 26 cycles in each run. The mutated gene was then obtained in two pieces, which were isolated by agarose gel electrophoresis. This was followed by purification with the QIAquick Gel Extraction Kit. In the second step, the two gene fragments were used as templates in the reaction mixture, heated to 95 °C prior to the addition of the Vent polymerase. The temperature was then lowered to 55 °C when the complementary ends of the two DNA portions formed double-stranded DNA. The complementary strands were synthesized during heating at 72 °C for 5 min. The complete strands were able to bind the terminal primers (5′- and 3′-primers to the 5′- and 3′-termini of the gene, respectively), which were added to the mixture at 95 °C. The amplification was then carried out in 30 cycles at 95, 54, and 72 °C for 1, 1, and 2.5 min, respectively. The PCR product was identified on an agarose gel (1%) and purified with a QIAquick kit. The pure product was digested with *Eco*RI and *Sal*I restriction enzymes and isolated with agarose gel electrophoresis. After purification from the gel, it was ligated into an empty pBluescript SK vector digested with *Eco*RI and *Sal*I enzymes. The Tyr452Phe mutation was verified by digestion with the *Bam*HI enzyme. The expression and purification of the Tyr452Phe variant were the same as for the wild-type oligopeptidase B.

Polyhistidine-Tagged Enzymes. The gene of oligopeptidase B was isolated from the pSKOpB construct (*24*) by the two-step PCR method described above. We created an *Nde*I restriction site at the 5′-end of the coding region with the primer 5′-GACATTCCATATGCTACCAAAAGCCGCCCG-3′ (*Nde*I site underlined) and a *Bam*HI restriction site at the 3′-end of the coding region with the primer 5′-ACTAGGATCCTTAATAACCTGGACAGCATGA-3′ (*Bam*HI site underlined). A primer pair was also designed at the 1753th nucleotide position to eliminate an inner *Bam*HI site.

These primers are the 5′-GTAACCCGCAaGAcCCG-CAATATTAC-3′ sense mutagenic primer and the 3′-CATTGGGCGTtCTgGGCGTTATAATG-5′ antisense mutagenic primer (the altered *Bam*HI site underlined). The two-step PCR was carried out as described for the Tyr473Phe mutant of prolyl oligopeptidase (*23*). The PCR product was identified on an agarose gel (1%) and purified with a QIAquick kit. The pure product was digested with *Nde*I and *Bam*HI restriction enzymes and isolated with agarose gel electrophoresis. After purification from the gel, it was ligated into an empty pET-15b vector, digested with *Nde*I and *Bam*HI enzymes. The gene for oligopeptidase B was in frame with a polyhistidine tag in the pET-15b vector, and so the polyhistidine tail was added to the N-terminus of the protein. The tag contained a thrombin cleavage site that permitted removal of the polyhistidine tail.

The Tyr452Phe mutant of the oligopeptidase B gene with the polyhistidine tail was constructed by cloning, using the *Sma*I restriction site at nucleotide position 1043, and the *Nsi*I site at nucleotide position 1543 of the gene. This 500-nucleotide segment contained the Tyr452Phe mutation, which was cleaved from the pSKOpB/Y452F vector by sequential digestion with *Sma*I and *Nsi*I restriction enzymes, purified by agarose gel electrophoresis, extracted from the gel with the QIAquick Gel Extraction Kit (QIAGEN), and ligated to the place of the *Sma*I−*Nsi*I fragment of the wild-type oligopeptidase B gene the in pET-15b plasmid. The ligation mixtures were transformed into *E. coli* DH5α cells, and from the colonies grown on LB was isolated the DNA. The presence of the insert in the plasmid was justified by digestion with *Nde*I and *Bam*HI enzymes. The Tyr452Phe

mutant had an extra *Bam*HI site, which was introduced upon creation of the mutation.

The tagged enzymes were expressed in *E. coli* BL21-(DE3)pLysS. After transformation, the cells were grown in 2 × 500 mL of LB, shaking with 250 rpm at 37 °C until the OD_{600} reached a value of 0.6. Then 1 mM isopropyl β-D-thiogalactopyranoside was added, and the medium was incubated overnight at 30 °C. The cells were harvested by centrifugation and suspended in 30 mL of binding buffer [5 mM imidazole, 0.2 M NaCl, and 20 mM Tris (pH 8.0)]. The suspension was sonicated on ice and centrifuged for 30 min at 20000*g*. The supernatant was loaded onto a Ni^{2+} chelation column (25 mL), Ni−NTA Superflow (QIAGEN) in an FPLC system, and purified according to the protocol of the manufacturer. The enzyme proved to be at least 90% pure, as indicated by SDS−polyacrylamide gel electrophoresis. Further purification was achieved by chromatography on a Mono Q column, using the FPLC system.

Kinetics. The specificity rate constants (k_{cat}/K_m) were determined under first-order conditions, i.e., at substrate concentrations lower than K_m. The first-order rate constant was divided by the total enzyme concentration to provide k_{cat}/K_m. For the specificity studies, the following internally quenched fluorescence substrates were prepared by solid phase synthesis (the scissile bonds in the peptides are marked):

Substrate RR: Abz-Thr-Arg-Arg-|-Phe(NO_2)-Ser-Leu-NH_2

Substrate CR: Abz-Thr-Cit-Arg-|-Phe(NO_2)-Ser-Leu-NH_2

Substrate RC: Abz-Thr-Arg-|-Cit-Phe(NO_2)-Ser-Leu-NH_2

Substrate CC: Abz-Thr-Cit-Cit-Phe(NO_2)-Ser-Leu-NH_2

The reactions were monitored fluorometrically at 25 °C by using a Cary Eclipse fluorescence spectrophotometer equipped with a Peltier four-position multicell holder and a temperature controller. The excitation and emission wavelengths were 337 and 420 nm, respectively, in a four-component buffer with a constant ionic strength (*25*), composed of 25 mM glycine, 25 mM acetic acid, 25 mM Mes, and 75 mM Tris and containing 1 mM EDTA (standard buffer). The buffer was titrated to the desired pH with HCl or NaOH, and slight changes in the ionic strength were adjusted by the addition of NaCl. At a low enzyme concentration (<10 nM), the buffer was supplemented with 1 μM bovine serum albumin.

Theoretical curves for bell-shaped pH−rate profiles were calculated by nonlinear regression analysis, using eq 1 and the GraFit software (*26*).

$$k_{cat}/K_m = k_{cat}/K_m(\text{limit})[1/(1 + 10^{pK_1-pH} + 10^{pH-pK_2})] \quad (1)$$

where k_{cat}/K_m(limit) stands for the pH-independent maximum rate constant, and K_1 and K_2 are the dissociation constants of a catalytically competent base and acid, respectively. At low ionic strength, two additional ionizing groups modify the bell-shaped character of the pH dependence curve. The resulting pH−rate profile conforms to eq 2

$$k_{cat}/K_m = k_{cat}/K_m(\text{limit})_1[1/(1 + 10^{pK_1-pH} + 10^{pK_1+pK_x-2pH} + 10^{pH-pK_y})] + k_{cat}/K_m(\text{limit})_2[1/(1 + 10^{pK_y-pH} + 10^{pH-pK_2})] \quad (2)$$

where the limiting values stand for the pH-independent maximum rate constants for the two active forms of the enzyme and K_1, K_x, K_y, and K_2 are the dissociation constants of four enzymatic groups whose state of ionization controls the reaction. When the effect of K_y is not seen, eq 3 is used.

$$k_{cat}/K_m = k_{cat}/K_m(\text{limit})[1/(1 + 10^{pK_1-pH} + 10^{pK_1+pK_x-2pH} + 10^{pH-pK_2})] \quad (3)$$

When a substrate binds in an alternative unreactive mode, which is competitive with the reactive binding mode, the Michaelis−Menten equation changes to eq 4

$$v = V[S]/(K_m + [S] + [S]^2/K_{is}) \quad (4)$$

where K_{is} is the inhibition constant for the second substrate.

The K_i values, the dissociation constants of the enzyme−inhibitor complex, were calculated from eq 5.

$$k_i/k_0 = 1/(1 + [I]/K_i) \quad (5)$$

where k_i and k_0 are pseudo-first-order rate constants determined at substrate concentrations of $<0.1K_m$ in the presence and absence of inhibitor (I), respectively.

The thermodynamic parameters were calculated from Eyring plots (eq 6)

$$\ln(k/T) = \ln(R/N_A h) + \Delta S^*/R - \Delta H^*/RT \quad (6)$$

where k is the rate constant, R is the gas constant (8.314 J mol^{-1} K^{-1}), T is the absolute temperature, N_A is Avogadro's number (6.022×10^{23} mol^{-1}), h is Planck's constant (6.626×10^{-34} J s^{-1}), the enthalpy of activation $\Delta H^* = -(\text{slope}) \times 8.3 \times 14$ J/mol, and the entropy of activation $\Delta S^* = (\text{intercept} - 23.76) \times 8.3 \times 14$ J mol^{-1} K^{-1}. The free energy of′ activation, ΔG^*, was calculated from eq 7.

$$\Delta G^* = \Delta H^* - T\Delta S^* \quad (7)$$

RESULTS AND DISCUSSION

Electrostatic Effects Control Substrate Binding. A pair of basic residues in the substrate is crucial for the specific hydrolysis carried out by oligopeptidase B. Increased salt concentrations mask electrostatic interactions that may occur in the complexes formed between oligopeptidase B and its substrates (*19*, *27*). To investigate substrate recognition, which is an essential feature of drug design, we have examined the effects of ionic strength on the hydrolysis of substrates containing a single arginine or a pair of arginine residues. To this end, we have prepared the closely related oligopeptide substrates RR, CR, and RC (see Experimental Procedures), having a real scissile peptide bond rather than a relatively good leaving group, such as Amc or Nap, previously used in kinetic investigations. Substitution of citrulline for arginine in substrate RR was chosen because the side chains of arginine and citrulline are of similar size, but citrulline does not have a positive charge that seems to be essential for the specificity of oligopeptidase B, as

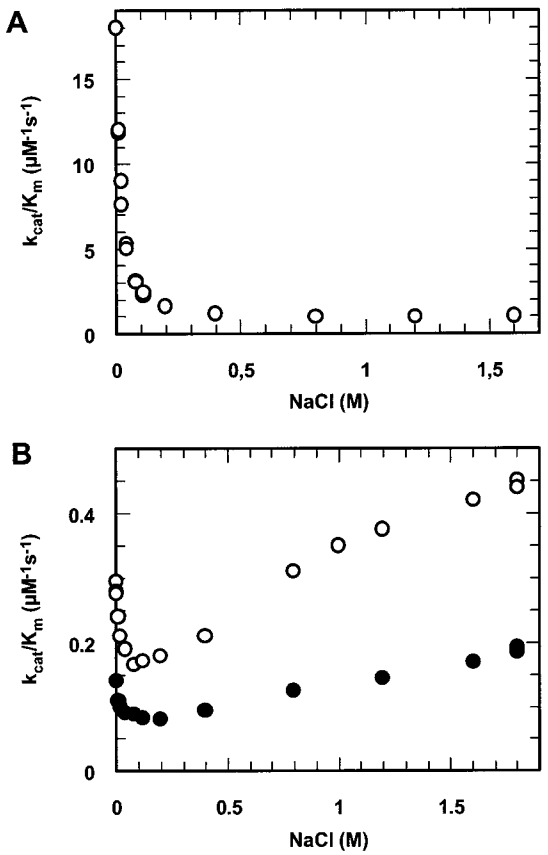

FIGURE 1: Effects of NaCl concentration on rate constants for oligopeptidase B. (A) Substrate RR measured at 0.4−3 nM enzyme. (B) Substrates CR (○) and RC (●) both measured with 40−80 nM enzyme. The reactions were assessed at pH 8.0, and the concentrations were 0.5 μM for each substrate.

indicated by its much slower reaction with Bz-Cit-Et than with Bz-Arg-Et (*27*). Indeed, we have found that the specificity rate constant for substrate CC (see Experimental Procedures) is only 0.01 mM^{-1} s^{-1}, while those for substrates RR, CR, and RC are 5700, 280, and 140 mM, respectively, measured at the pH optima.

Figure 1A shows that the specificity rate constant (k_{cat}/K_m) for substrate RR sharply diminishes with an increase in NaCl concentration. The marked reduction in the rate constant can be rationalized in terms of depressing the electrostatic attractions between the enzyme and substrate. By contrast, the salt effects on substrates CR and RC are less pronounced and provide minimum curves (Figure 1B), indicating that two different effects prevail over the broad range of NaCl concentrations. In the region of low ionic strength, the rate constant decreases with increasing salt concentration, but the effect is significantly lower in magnitude than that found with the substrate containing two basic residues. The increase in rate at high ionic strength is similar to that observed for the reaction of prolyl oligopeptidase with neutral substrates (*23*). The similar behaviors of substrates CR and RC suggest that the arginine residues of both peptides bind to the same S1 site, possibly to enzymatic carboxylate ions (to be discussed later). In fact, amino acid sequence analysis of the reaction products has shown that the cleavage occurred in both peptides at the carbonyl group of the arginine residue. These results indicate that substrates with one arginine prefer subsite S1 to S2.

We have also examined the cleavage site in substrate RR. Interestingly, an extensive hydrolysis of the compound gave three fragments, Abz-Thr-Arg-Arg-OH, Abz-Thr-Arg-OH, and Phe(NO_2)-Ser-Leu-NH_2, suggesting that the enzyme cleaved the substrate at two different sites or that the first product, Abz-Thr-Arg-Arg-OH, underwent a further cleavage. However, since an Arg-Phe(NO_2)-Ser-Leu-NH_2 fragment was not found, substrate RR obviously did not split between the two arginine residues, but the Abz-Thr-Arg-OH fragment should come from the secondary cleavage of Abz-Thr-Arg-Arg-OH. This was confirmed by investigations into the kinetics of the formation of reaction products, which demonstrated that only two products appeared at 25, 50, and 90% of the hydrolysis, and the third product emerged during further incubation after the complete breakdown of the substrate. This indicates that the two arginines of the Abz-Thr-Arg-Arg-OH peptide may also bind at the S1 and S1′ subsites; however, the probability of this binding is rather low, so its effect can be neglected in the kinetic investigations.

The possibility that the substrate arginines bind to enzymatic carboxyl groups has been analyzed with the aid of the oligopeptidase B model built on the basis of the known structure of prolyl oligopeptidase (*28*). According to the model, the P2 arginine residue of Z-Arg-Arg-OH was bound to the carboxyl groups of Asp460 and Asp462. In the related prolyl oligopeptidase, the P1 proline residue is stacked with the indole ring of Trp595, which is the counterpart of Glu576 of oligopeptidase B. Hence, Glu576 may constitute the S1 binding site. Moreover, Glu576 and its neighboring Glu578 presumably form a carboxyl dyad similar to that of the Asp460 and Asp462 pair at subsite S2. Examination of the positions of the corresponding amino acid residues of prolyl oligopeptidase (Thr481/Asn483 and Trp595/Thr597) reveals that the side chains point to the right directions. Recent site-specific mutagenesis studies strongly support the participation of the two dyads in substrate binding (R. Morty and N. Andrews, Yale University, New Haven, CT, unpublished observation). The importance of the carboxyl dyads in the binding of the arginine side chain is consistent with the results obtained with furin, another processing enzyme, which cleaves at a pair of basic residues. The structure of furin is related to subtilisin, but the binding site of furin contains several carboxyl groups that bind the substrate arginines (*29*).

The S2 Subsite Is Implicated in Substrate Inhibition. In the reaction of oligopeptidase B with substrate RR, an alteration in ionic strength modifies primarily the K_m rather than the k_{cat}. The 5-fold increase in K_m in the presence of 1.0 M NaCl is consistent with the weakening of binding (Table 1). Furthermore, the binding of a substrate containing a pair of arginine residues (substrate RR) is much stronger, and the K_m is lower than that of a substrate with one arginine (substrates CR and RC). We could determine the dissociation constant of the enzyme−substrate complex (K_s) for the poor substrate CR by measuring the inhibition constant ($K_i \approx K_s$) against the activity of a highly specific substrate, Z-Arg-Arg-Amc, using eq 5 (*30*). Under different conditions, K_i was lower by a factor of 2−3 relative to K_m, which indicates that K_m is characteristic of the binding constant.

Determination of K_m was complicated with substrate inhibition observed with peptide RR (Figure 2 and Table 1). This implies the binding of two substrate molecules to

Table 1: Kinetic Parameters for the Reactions of Oligopeptidase B[a]

	K_m (μM)	K_{is} (μM)	k_{cat} (s^{-1})	k_{cat}/K_m (μM^{-1} s^{-1})
$I = 1.0$ M				
substrate RR				
15 °C	14.0 ± 3.0	100 ± 26	8.6 ± 1.1	0.570
15 °C[b]	12.8 ± 3.3		7.8 ± 0.9	0.572
25 °C	24.0 ± 4.1	125 ± 26	23.2 ± 2.3	0.965
25 °C[b]	18.2 ± 2.3		18.7 ± 1.2	1.030
35 °C	37.9 ± 4.3	131 ± 18	23.6 ± 1.7	0.730
35 °C[b]	31.7 ± 4.4		19.8 ± 1.6	0.733
substrate CR				
25 °C[b]	80.0 ± 9.2		20.3 ± 1.0	0.234
substrate RC				
25 °C[b,c]	29.8 ± 2.1		4.90 ± 0.18	0.164
$I = 3$ mM				
substrate RR				
25 °C	4.8 ± 0.6	42 ± 8	21.0 ± 1.5	4.312
25 °C[b]	4.0 ± 0.7		18.2 ± 1.9	4.516
substrate CR				
25 °C[b,c]	83.0 ± 7.7		23.9 ± 1.5	0.288 (0.293)[e]
25 °C[b–d]	38.2 ± 3.4		35.8 ± 2.1	0.938 (0.893)[e]
substrate RC				
25 °C[b,c]	38.3 ± 2.5		6.73 ± 0.27	0.175

[a] At pH 8.0. [b] Calculated from the front region of the curve (see the filled symbols in Figure 2). [c] Substrate inhibition at high substrate concentrations did not fit eq 4. [d] In the presence of 7 mM $CaCl_2$ without EDTA. [e] The value in parentheses was measured under first-order conditions.

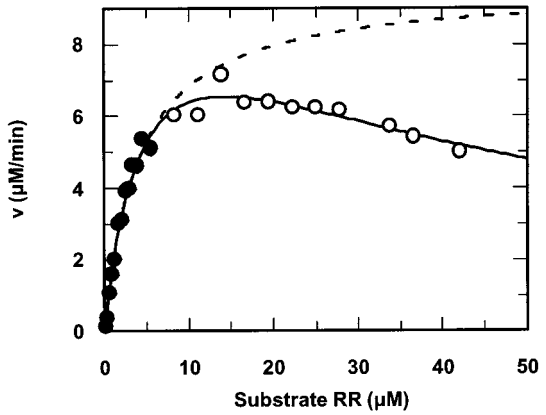

FIGURE 2: Inhibition of the activity of oligopeptidase B at enhanced substrate concentrations. Initial rates were measured in the standard buffer (pH 8.0, $I = 3$ mM), with 0.17 nM enzyme, using variable concentrations of substrate RR at 25 °C. The curve was calculated with eq 4. The dashed line fitted to the black symbols was calculated with the Michaelis−Menten equation.

the enzyme, resulting in an ineffective complex. Using eq 4, we could calculate both the K_m and the second dissociation constant, K_{is}, that was higher by 1 order of magnitude than K_m. This rendered it possible to calculate the parameters from the Michaelis−Menten equation, too, using the lower substrate region. The K_m values calculated from a partial data set (black symbols in Figure 2) and the whole data sets agreed within experimental error (Table 1). Moreover, the k_{cat}/K_m calculated by dividing k_{cat} by K_m agreed with the k_{cat}/K_m measured under first-order conditions (not shown).

To exclude inner filter effects that could result in an apparent substrate inhibition, we have checked the linearity of the fluorescence intensity with increasing substrate concentration. Corrections for the inner filter effect were made at high substrate concentrations. The validity of substrate inhibition was also demonstrated by spectrophotometrically assessing the hydrolysis of the Bz-Arg-Nap

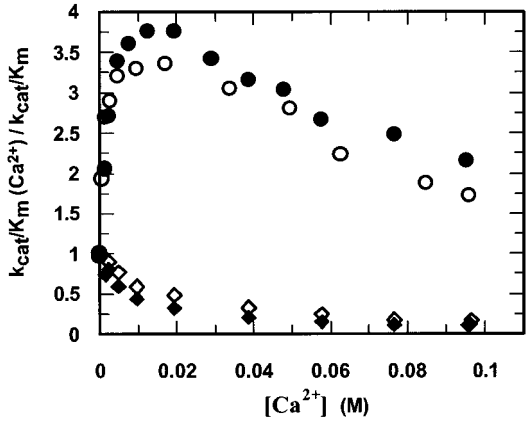

FIGURE 3: Effects of $CaCl_2$ on the activity of oligopeptidase B. The reactions were carried out in the standard buffer (pH 8.0, $I = 2$ mM), without the addition of EDTA. The enzyme concentrations were 0.5−3 nM for substrate RR (◇), 2−10 nM for substrate CR (○), 0.07−0.2 nM for Z-Arg-Arg-Amc (◆), and 2−4 nM for Bz-Arg-Nap (●).

Table 2: Effects of $CaCl_2$ on Oligopeptidase B Reactions

	substrate RR k_{cat}/K_m (μM^{-1} s^{-1})	Bz-Arg-Nap k_{cat}/K_m (μM^{-1} s^{-1})
without added salt	7.59 (100%)	0.408 (100%)
0.1 M $CaCl_2$	1.30 (17%)	0.875 (214%)
0.2 M NaCl	1.65 (22%)	0.278 (68%)

substrate at 338 nm, in which case the inner filter effect was eliminated. The fluorescence and spectrophotometric methods gave similar results. The substrate inhibition was also observed with Bz-Arg-Nan measured spectrophotometrically at 410 nm.

In contrast to substrate RR, substrates CR and RC produced a different type of substrate inhibition that failed to conform to eq 4. Apparently, the inhibition by substrates CR and RC did not follow the uncompetitive mechanism implied by eq 4. When the participation of four carboxyl groups at the active site is considered, the substrates with a single arginine have more alternative binding modes than substrate RR that occupies both the S1 and S2 subsites.

To test the nature of the potential carboxyl dyads, we have investigated the effect of Ca^{2+}, as this ion requires two neighboring carboxylate groups to balance the two positive charges. Hence, the catalytic activity of oligopeptidase B bearing carboxyl dyads as binding sites may be influenced by relatively low concentrations of Ca^{2+}. Figure 3 shows that the reactions of substrate RR and Z-Arg-Arg-Amc are inhibited with the increasing concentration of $CaCl_2$, as observed with NaCl. The level of inhibition is ∼80% at both 0.1 M $CaCl_2$ and 0.2 M NaCl, having the same ionic strength (Table 2). In contrast, the Bz-Arg-Nap reaction is still activated in 0.1 M $CaCl_2$ (215% activity), but inhibited in 0.2 M NaCl (68% activity). It can be seen in Figure 3 that substrates with a single arginine residue (substrate CR and Bz-Arg-Nap) are significantly activated at $CaCl_2$ concentrations as low as 5−10 mM, but the activity tends to decrease when the $CaCl_2$ concentration is further increased. Similar results were obtained with $MgCl_2$ (not shown). A possible explanation of this phenomenon may be that blocking of the S2 site by Ca^{2+} reduces the improper binding modes of the substrate having a single arginine. Indeed, the major change by 5 mM $CaCl_2$ is caused in the K_m value, suggesting a

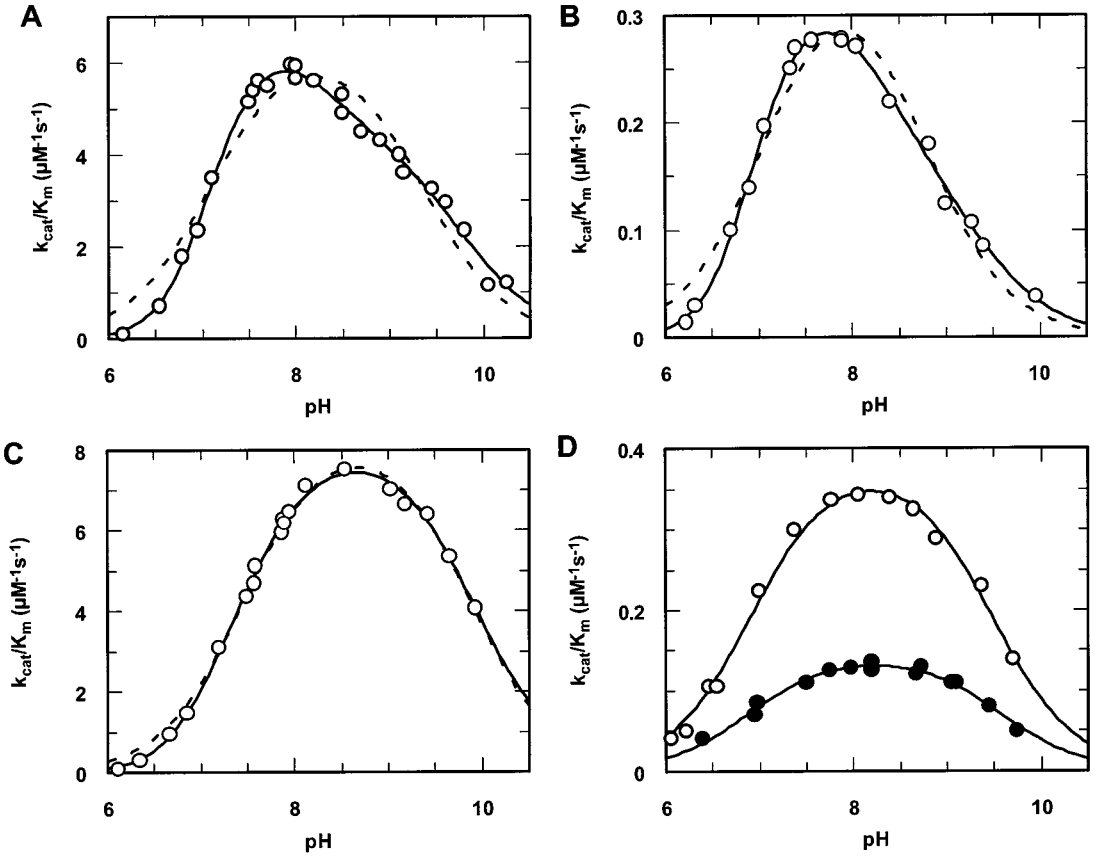

FIGURE 4: pH−rate profiles for the reactions of oligopeptidease B. (A) Substrate RR was measured at 4−18 nM at $I = 3$ mM. The ionic strength was strictly maintained throughout the pH range. The points were fitted to eq 2. The broken line represents a bell-shaped curve (eq 1). (B) Substrate CR was measured at 60−120 nM enzyme at $I = 3$ mM. The points were fitted to eq 2. The broken line represents a bell-shaped curve (eq 1). (C) Substrate RR measured in the presence of 5 mM $CaCl_2$ at enzyme concentrations of 1−8 nM. The substrate concentrations were in all cases 0.5 μM. The points were fitted to eq 3. The broken line represents a bell-shaped curve (eq 1). (D) Substrate CR was measured at 10−21 nM enzyme (○) and substrate RC measured at 30−60 nM enzyme (●) in the presence of 1 M NaCl. The data fit to eq 1.

stronger binding, while k_{cat} increases to a lesser extent (substrate CR in Table 1). Both alterations enhance the k_{cat}/K_m value, which indicates that the detrimental effect of the S2 site on substrate binding is substantially depressed. On the other hand, substrates with a pair of basic residues exploit both subsites and bind stronger than Ca^{2+} so that only the inhibitory effect of $CaCl_2$ prevails.

The role of subsite S2 is of particular importance, as it not only enhances the specificity for a pair of arginines but also by diminishing the specificity for a single arginine can further discriminate between the substrates bearing one or two basic residues. Such a function of the second subsite has not been recognized so far; although this novel aspect of substrate recognition is not a major issue only with processing enzymes, which cleave at two basic residues, it could be a general phenomenon in enzymology.

A Subsite Carboxyl Group Perturbs the pH−Rate Profiles. It has previously been shown that the pH dependence of k_{cat}/K_m for the hydrolysis of Z-Arg-Arg-Amc and Bz-Arg-Nap by oligopeptidase B is more complicated at low ionic strengths than the simple bell-shaped curve found with the classic serine peptidases, while in the presence of 1 M NaCl, the data fairly well conform to a bell-shaped profile (*19*, *27*). Panels A and B of Figure 4 illustrate the pH−k_{cat}/K_m profiles of hydrolysis of genuine peptide bonds (substrates RR and CR, respectively) in the absence of added NaCl. It can be seen that the rate constants do not fit to a regular bell-shaped curve (eq 1). The low-pH limb is significantly steeper than that anticipated for the dissociation of a single base, indicating that two groups ionize in that region (pK_1 and pK_x of eq 2). The alkaline region of the curve is also affected by an additional ionizing group (pK_y), which transforms the single bell-shaped curve into a double bell-shaped profile. The two terms of eq 2 actually describe two enzyme forms with different activities, which are characterized by k_{cat}/K_m(limit)$_1$ and k_{cat}/K_m(limit)$_2$, as discussed previously (*27*).

The parameters of the pH dependence curves of panels A and B of Figure 4 are shown in Table 3. Because of the six parameters of eq 2, the errors are relatively large. To illustrate the better adherence of the data to eq 2, a simple bell-shaped curve (eq 1) is also fitted to the points (Figure 4A,B). The two ionizing groups associated with the low-pH limb very likely refer to the catalytic histidine (pK_1) and a carboxyl group (pK_x) implicated in substrate binding. The involvement of the carboxyl group is strongly supported by Figure 4C, illustrating that in the presence of 5 mM $CaCl_2$ the data fit fairly well to a bell-shaped curve rather than to the complex pH dependence found without $CaCl_2$ (Figure 4A). Apparently, the pK_x value practically disappears when the carboxyl group reacts with the Ca^{2+} ion, although a little effect is still discernible at low pH. It should be noted the pK_a values extracted from the pH dependence of k_{cat}/K_m are characteristic of the ionizing groups of the free enzyme. Therefore, they are independent of whether the substrate arginine will bind

Table 3: Parameters for the pH Dependence Reactions of Oligopeptidasae B[a]

	substrate RR	substrate CR	substrate RC
$I = 3$ mM (eq 2)			
$k_{cat}/K_m(\text{limit})_1$ (mM^{-1} s^{-1})	7232 ± 946	351 ± 26	186 ± 20
$k_{cat}/K_m(\text{limit})_2$ (mM^{-1} s^{-1})	3879 ± 592	94 ± 60	49 ± 25
pK_1	6.99 ± 0.31	6.77 ± 0.20	7.04 ± 0.16
pK_x	6.87 ± 0.45	6.82 ± 0.28	6.06 ± 0.48
pK_y	8.28 ± 0.38	8.47 ± 0.28	8.35 ± 0.27
pK_2	9.84 ± 0.11	9.55 ± 0.40	9.71 ± 0.44
$I = 3$ mM (eq 1)			
k_{cat}/K_m(limit) (mM^{-1} s^{-1})	6710 ± 33	360 ± 21	166 ± 10
pK_1	7.05 ± 0.09	7.04 ± 0.08	7.00 ± 0.08
pK_2	9.40 ± 0.08	8.79 ± 0.08	8.85 ± 0.09
$I = 1$ M (eq 1)			
k_{cat}/K_m(limit) (mM^{-1} s^{-1})	1140 ± 33	383.3 ± 7.8	145.4 ± 2.7
pK_1	6.95 ± 0.07	6.90 ± 0.03	6.88 ± 0.04
pK_2	9.54 ± 0.06	9.49 ± 0.04	9.53 ± 0.04
$I = 2$ mM, 5 mM $CaCl_2$ (eq 1)			
k_{cat}/K_m(limit) (mM^{-1} s^{-1})	8481 ± 175	1482 ± 41	
pK_1	7.46 ± 0.03	7.45 ± 0.04	
pK_2	9.88 ± 0.04	9.58 ± 0.04	
$I = 2$ mM, 5 mM $CaCl_2$ (eq 3)			
k_{cat}/K_m(limit) (mM^{-1} s^{-1})	8230 ± 131	1435 ± 36	
pK_1	7.37 ± 0.03	7.34 ± 0.06	
pK_x	6.45 ± 0.17	6.43 ± 0.25	
pK_2	9.92 ± 0.03	9.62 ± 0.04	

[a] At 25 °C.

to the carboxylate ion during the catalysis. Accordingly, this carboxyl group may be assigned to either the S2 or the S1 site. From the pH dependence curve of substrate CR, the 5 mM $CaCl_2$ also eliminated the effect of pK_x. The parameters for the curves are included in Table 3. Besides the simple bell-shaped curve, the parameters for a sharper slope of the acidic limb are also shown.

The nature of the group with pK_y is unknown. It may not be directly involved in the catalysis; it may be located outside the active site. Indeed, the electrostatic effects of charged groups, even if they are remote from the active site, are able to influence the catalysis (*31*). Such an effect is observed with oligopeptidase B when the complex pH−rate profile is simplified to a bell-shaped curve in the presence of 1 M NaCl, which depresses electrostatic effects (Figure 4D and Table 1).

The group with pK_2 may reflect the decomposition of the active conformation of the enzyme. In fact, conformational changes do occur near pH 9 (*24*).

In addition to the changes observed in the pH−rate profiles, the values of the rate constants are also affected by the ionic strength. As seen from Table 3, masking two positive charges (substrate RR) causes a much greater effect on the rate constant than masking a single charge (substrates CR and RC).

The Catalytic Effects of the Oxyanion Binding Site Are Substrate-Dependent. It is generally assumed that the hydrogen bonds from the oxyanion binding site stabilize the transition state of the reaction (*20*−*22*). However, these hydrogen bonds may also influence the catalysis by interacting with the peptide carbonyl oxygen in the ground state. To examine the contribution of the oxyanion binding site to the catalysis, we have prepared the Tyr452Phe variant of oligopeptidase B lacking the critical OH group. The lack of the hydroxyl group did not cause a significant change in the physical properties of the protein: (i) The behavior of the enzyme variant during ion exchange chromatography in the FPLC system was identical with that of the wild-type peptidase. (ii) The fluorescence spectra of the wild type and the modified enzymes were identical within experimental error and agreed with that published earlier for the wild-type peptidase (*24*). (iii) The melting points determined with differential scanning calorimetry were also identical for the two enzymes (47.8 °C).

Table 4 shows the parameters of the pH dependence curves for various substrates. It is seen that the rate constants for the enzyme variant are lower by ∼2 orders of magnitude for most substrates. A major alteration, a difference of 3 orders of magnitude, is found with Bz-Arg-NH_2, indicating that the oxyanion binding site is more effective in the catalysis with the poor substrate than with a good substrate.

Unexpectedly, the reactions of the ester substrates are apparently not affected by the elimination of Tyr452 (Table 4). This holds with both the citrulline and arginine ester derivatives, although their kinetic specificities differ by 3 orders of magnitude. The lack of an effect on k_{cat}/K_m may readily be misinterpreted by assuming that the reaction with the better leaving group (alcohol vs amine) does not require electrophilic assistance, and that the oxyanion binding site is only important for substrates with poor leaving groups. However, determination of the Michaelis−Menten parameters for the Bz-Arg-Et reaction revealed a substantial difference between the wild-type enzyme and its variant as both k_{cat} and K_m decreased with the modified enzyme by the same factor of 120 (Table 5). The identical changes for k_{cat} and K_m are indicative of nonproductive binding, which implies an unreactive binding mode in competition with the reactive binding mode. In this case, k_{cat} is diminished since only a fraction of the substrate binds productively at saturation, and K_m is lowered because the additional binding mode results in an apparently stronger binding. Since k_{cat} and K_m are modified in a compensating manner, k_{cat}/K_m is not affected by nonproductive binding (*32*). Consequently, in addition to electrophilic catalysis, elimination of nonproductive binding may be another important role of the oxyanion binding site.

The decrease in both k_{cat} and K_m may alternatively be explained by stronger binding that diminishes K_m and by an elevated transition state that decreases k_{cat}. However, this possibility may require K_s to decrease by 2 orders of magnitude, while the binding determinant remains the same ionic interaction for both the wild type and the modified enzymes. Furthermore, it is not very likely that the different effects on k_{cat} and K_m would act exactly in a compensating manner, though this possibility cannot be excluded.

Oligopeptidase B has several subsites for binding large peptides tightly and specifically. A less specific small molecule, such as Bz-Arg-Et, may bind in different ways, but only one of the enzyme−substrate complexes is able to break down to products. Interestingly, nonproductive binding is not observed with the structurally related Bz-Arg-NH_2, which indicates that the amide hydrogen of Bz-Arg-NH_2 facilitates productive binding. However, this small molecule is still not a specific substrate, and requires the interaction with the Tyr452 OH group even in the ground state to be poised correctly for catalysis. This may explain why the specificity rate constant decreases in the absence of the tyrosine OH group by 3 orders of magnitude, more than that found with the better substrates.

Table 4: Effects of the Oxyanion Binding Site on the Kinetic Parameters[a]

	wild type (*A*)	Y452F variant (*B*)	*A*/*B*
substrate RR			
k_{cat}/K_m(limit) (mM^{-1} s^{-1})	1140 ± 33[b]	7.45 ± 0.39	153
pK_1	6.95 ± 0.07[b]	7.21 ± 0.08	
pK_2	9.54 ± 0.06[b]	9.64 ± 0.10	
substrate CR			
k_{cat}/K_m(limit) (mM^{-1} s^{-1})	383 ± 7.8[b]	1.63 ± 0.18	235
pK_1	6.90 ± 0.03[b]	7.08 ± 0.17	
pK_2	9.49 ± 0.04[b]	9.17 ± 0.20	
Z-Arg-Arg-Amc (I = 3 mM, eq 3)			
k_{cat}/K_m(limit) (μM^{-1} s^{-1})	27.8 ± 1.1	0.451 ± 0.011	61.6
pK_1	6.92 ± 0.11	7.16 ± 0.04	
pK_x	6.37 ± 0.34	6.57 ± 0.20	
pK_2	9.50 ± 0.07	9.52 ± 0.05	
Z-Arg-Arg-Amc			
k_{cat}/K_m(limit) (μM^{-1} s^{-1})	6.64 ± 0.25[c]	0.089 ± 0.003	74.6
pK_1	6.94 ± 0.07[c]	7.03 ± 0.06	
pK_2	9.60 ± 0.07[c]	9.63 ± 0.07	
Bz-Arg-Nap			
k_{cat}/K_m(limit) (mM^{-1} s^{-1})	597 ± 20	1.48 ± 0.03	403
pK_1	6.96 ± 0.06	7.19 ± 0.03	
pK_2	9.70 ± 0.08	9.56 ± 0.04	
Bz-Arg-NH_2			
k_{cat}/K_m (mM^{-1} s^{-1})[d]	107	0.052	2057
Bz-Arg-Et			
k_{cat}/K_m (mM^{-1} s^{-1})[d]	466	487	0.96
Bz-Cit-Et			
k_{cat}/K_m (M^{-1} s^{-1})[e]	600	180	3.3

[a] I = 1.0 M (eq 1). [b] From Table 3. [c] From ref *19*. [d] At pH 8.0. [e] At pH 7.0.

Table 5: Michaelis−Menten Parameters[a]

	wild type (*A*)	Y452F variant (*B*)	*A*/*B*
substrate RR			
k_{cat} (s^{-1})	18.7 ± 2.3	0.0538 ± 0.0012	348
K_m (μM)	18.2 ± 2.0	10.5 ± 0.5	1.73
k_{cat}/K_m (μM^{-1} s^{-1})	1.030	0.005	202
substrate CR			
k_{cat} (s^{-1})	20.3 ± 1.0	0.0511 ± 0.0022	397
K_m (μM)	80 ± 9.2	43.4 ± 4.0	1.84
k_{cat}/K_m (μM^{-1} s^{-1})	0.253	0.0011	230
substrate RC			
k_{cat}/K_m (μM^{-1} s^{-1})[b]	0.146	0.000559	262
Z-Arg-Arg-Amc			
k_{cat} (s^{-1})	19.3 ± 1.3	0.117 ± 0.005	165
K_m (μM)	5.3 ± 0.8	2.3 ± 0.3	2.3
k_{cat}/K_m (μM^{-1} s^{-1})	3.66	0.052	70
Bz-Arg-Et			
k_{cat} (s^{-1})	78.1 ± 7.1	0.671 ± 0.015	116
K_m (μM)	167 ± 17	1.38 ± 0.17	121
k_{cat}/K_m (μM^{-1} s^{-1})	0.466	0.487	0.96

[a] At 25 °C, pH 8.0, and 1.0 M NaCl. [b] Measured under first-order conditions.

A small amount of oligopeptidase B is constitutively produced in *E. coli*. This wild-type enzyme may be included in the preparations of enzyme variants since the separation of two virtually identical molecules is extremely difficult. Because the wild-type enzyme displays much higher activity than the enzyme variant, a very small amount of the residual wild-type enzyme could seriously interfere with kinetic studies. Therefore, we have prepared both the wild-type enzyme and the Tyr452Phe variant linked with a polyhistidine tag. After purification on a Ni^{2+} column, the wild-type enzyme with and without the polyhistidine tag gave identical activities, indicating that the polyhistidine tag does not affect the catalytic activity. In the case of the Tyr452Phe variant, some preparations exhibited slightly higher activity without the polyhistidine tag than that bearing the label. Therefore, the kinetic parameters given in Tables 4 and 5 were determined with the Tyr452Phe variant coupled with the polyhistidine tag. Removal of the polyhistidine tag by digestion with thrombin did not influence the activity.

Titration of Oligopeptidase B with Inhibitors Separates the Overlapping pK_a Values Associated with the Acid Slope of the pH Dependence Curves. From the complex pH−rate profile (Figure 4A), the true pK_a of the catalytic histidine cannot be extracted. However, the pK_a may be titrated with a product-like inhibitor having a free C-terminal carboxyl group. Specifically, recent X-ray crystallographic studies on the structurally related prolyl oligopeptidase demonstrated that the free carboxylate ion of Z-Gly-Pro-OH formed a salt bridge with the active site histidine. It was found that the association constant ($1/K_i$) of the product-like inhibitor increased with decreasing pH, as the catalytic histidine became protonated (*33*). The histidine titrated according to a simple dissociation curve that was characterized by a pK_a of 6.2.

To titrate the catalytic histidine of oligopeptidase B, we have prepared acetyl-Thr-Arg-Arg-OH, which proved to be a specific product-like inhibitor. The rate constants were determined at increasing concentrations of inhibitor, and the K_i values were calculated according to eq 5. The results have shown distinct a pH dependence for $1/K_i$ (Figure 5). Instead of the simple dissociation, a sharp bell-shaped curve was obtained, indicating that the protonation of some group counteracts the inhibitor binding at low pH (Table 6). The two pK_a values are as close as 0.8 unit. The higher pK_a (∼7.3) extracted from the curve of Figure 5 should be associated with the imidazole ionization, and the lower pK_a (∼6.5) likely

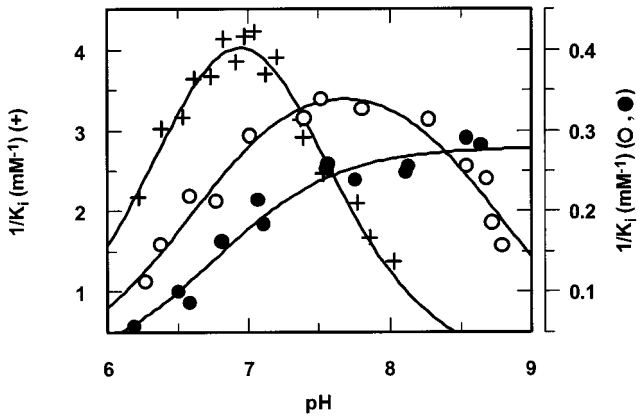

FIGURE 5: Titration of oligopeptidase B with inhibitors. The reactions were assessed with acetyl-Thr-Arg-Arg-OH at $I = 3$ mM (+) and benzamidine at $I = 3$ mM (○) and with the addition of 1.0 M NaCl (●). The inhibition constants (K_i) were calculated from eq 5. The parameters of the curves are shown in Table 6.

Table 6: pH Dependence of the Association Constants for Acetyl-Thr-Arg-Arg-OH and Benzamidine Complexed with Oligopeptidase B and Its Tyr452Phe Variant[a]

	wild type	Y452F variant
acetyl-Thr-Arg-Arg-OH		
$1/K_i$(limit) (mM^{-1})	7.43 ± 0.71	3.70 ± 0.34
pK_1	6.56 ± 0.08	6.47 ± 0.09
pK_2	7.31 ± 0.08	7.56 ± 0.08
benzamidine		
$1/K_i$(limit) (mM^{-1})	0.395 ± 0.021	nd[c]
pK_1		6.60 ± 0.07
pK_2		8.76 ± 0.08
benzamidine[b]		
$1/K_i$(limit) (mM^{-1})	0.279 ± 0.008	0.195 ± 0.008
pK_a	6.75 ± 0.06	6.63 ± 0.09

[a] The reactions were assessed at $I = 3$ mM. [b] $I = 1.0$ M. [c] Not determined.

refers to one of the carboxylate ions involved in the arginine binding. The pK_a of 6.5 is a reasonable value for a carboxyl group, which is located in the environment of another negative charge that stabilizes the protonated form of the carboxyl group. These two pK_a values are probably related to those extracted from the pH−k_{cat}/K_m profile of substrate RR (7.0 and 6.9). Indeed, if fitting is achieved with eq 2, in which pK_1 was set to a constant value of 7.3 (the value obtained from titration), the resulting pK_x is 6.4, and the resulting curve is identical, within experimental error, to that obtained in Figure 4A with the original parameters (7.0 and 6.9). Hence, the less precise data obtained from the complex pH−rate profile shown in Figure 4A (see the standard errors in Table 3) are consistent with the more exact values derived from the bell-shaped titration curve (Figure 5 and Table 6). Of course, it is much easier to evaluate the pK_a values of a bell-shaped curve than to separate overlapping ionizations of the two bases (carboxylate ion and imidazole base) associated with the acidic slope of the pH−rate profiles. Nevertheless, using the simpler eq 3 in the presence of 5 mM $CaCl_2$ (Table 3), the pK_a values extracted from the pH dependence curve agree well with those obtained from the titration experiment.

The distinctive pH dependence of $1/K_i$ for benzamidine further supports the idea that we really titrate the catalytic histidine (Figure 5). This compound does not possess a carboxyl group that would be able to form a salt bridge with the protonated histidine. Indeed, it gives a much wider pH dependence curve under the conditions employed for the titration with Ac-Thr-Arg-Arg-OH. In the presence of 1.0 M NaCl, $1/K_i$ does not decrease in the alkaline pH region, but fits to a simple dissociation curve, indicating that the enzymatic carboxylate ion proposed to be involved in the binding of Ac-Thr-Arg-Arg-OH (Figure 5) is also implicated in the binding of benzamidine. As expected, the binding of Ac-Thr-Arg-Arg-OH is much stronger; $1/K_i$ is 19 times higher than that of benzamidine (Table 6).

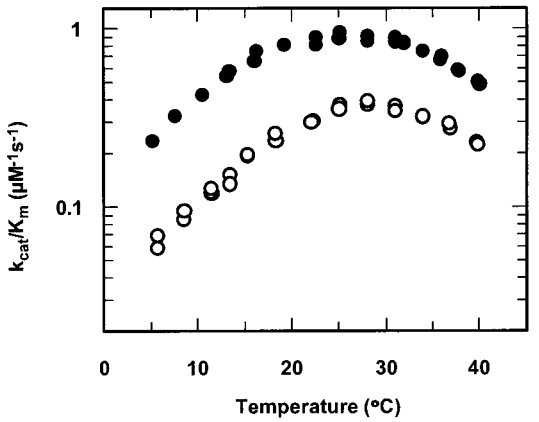

FIGURE 6: Temperature dependence of k_{cat}/K_m for oligopeptidase B reactions. The reactions were carried out at pH 8.0 in the presence of 1 M NaCl with substrates RR (●) and CR (○). The *Y*-axis is shown in logarithmic scale. The enzyme concentrations were 3−8 nM and 10−42 nM for substrates RR and CR, respectively.

Titration of the Tyr452Phe variant has also been carried out, using the Ac-Thr-Arg-Arg-OH inhibitor. The pK_a value for the variant is similar within experimental error to that obtained with the wild-type enzyme (Table 6). However, the association constant is somewhat smaller, indicating that in the complex of the wild-type enzyme a weak hydrogen bond is formed between the tyrosine side chain and the carbonyl oxygen of the inhibitor.

The Abnormally Low Temperature Optimum May Be Caused by the Disruption of the Hydrogen Bond Formed between the Enzyme and the NH Group of the Scissile Peptide Bond. The temperature dependence of the specificity rate constant for the reaction of oligopeptidase B with amide substrates is unusual as k_{cat}/K_m decreases above 25 °C, much below the physiological temperature, while with Bz-Arg-Et the temperature dependence of the reaction is normal (*27*). The peptide substrates RR and CR also display low temperature optima for k_{cat}/K_m (Figure 6), just like substrate RC (not shown). A similar phenomenon was observed with thrombin, and the results were interpreted in terms of changes in the rate-limiting step as a function of temperature (*34*). Such studies offer a possibility for the determination of the individual rate constants included in the composite constants [$k_{cat} = k_2k_3/(k_2 + k_3)$ and $k_{cat}/K_m = k_1k_2/(k_{-1} + k_2)$], as well as the corresponding activation energies, provided that the reaction proceeds through the simple acyl−enzyme mechanism:

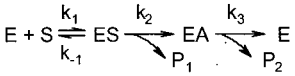

where k_1 is the second-order rate constant for formation of the enzyme−substrate complex (ES), the complex dissociates

Table 7: Thermodynamic Parameters for the Oligopeptidase B Reactions[a]

substrate, enzyme[b]	ΔH^* (kJ mol^{-1})	ΔS^* (J mol^{-1} K^{-1})	ΔG^* (kJ mol^{-1})
RR, Wt	62.8	84.4	37.6
RR, YF	65.1	49.5	50.3
RR, Wt[c]	67.5	114.6	33.3
CR, Wt	70.9	101.9	40.5
CR, YF[d]			
RC, Wt	59.0	59.0	41.4
RC, YF[d]			

[a] At 25 °C, pH 8.0, and $I = 1.0$ M. [b] Wt, wild-type enzyme; YF, Tyr452Phe variant. [c] $I = 3$ mM. [d] A linear Eyring plot was not obtained (see Figure 7).

at a rate k_{-1} or forms an acyl−enzyme intermediate (EA) at a rate k_2, and the acyl−enzyme intermediate hydrolyzes with the deacylation rate constant k_3. The substrate decomposes into two products, P1 and P2, during the reaction.

The above method (*34*) was applied to our system with different substrates (RR and CR) under different conditions (with and without 1.0 M NaCl). However, we did not obtain acceptable values for the rate constants; i.e., the data points failed to conform to the theoretical curve predicted by the calculated parameters, which were extracted from the linear parts of the temperature dependence. This indicates that the maximum of the temperature dependence curve cannot be interpreted in terms of the different changes in k_2 and k_{-1} with the increase in temperature. This inference is supported by the similar temperature dependence of the wild-type enzyme and of the Tyr452Phe variant. Specifically, k_2 decreases dramatically in the enzyme variant, which is not expected for k_{-1}. If this mechanism applied, the reactions of the wild-type enzyme and its variant would exhibit distinct temperature dependencies, contrary to our finding.

The maximum of the temperature dependence may be rationalized in terms of alteration in the structure of the enzyme−substrate complex. The maximum was observed with all peptide and amide substrates, but not with esters. Hence, we may assume that the NH group of the leaving portion should form a hydrogen bond with the enzyme or within the substrate molecule, and this interaction breaks down with increasing temperature.

The Reaction Barrier Is Entropic at Physiological Temperatures. From the low-temperature region of the reaction of wild-type oligopeptidase B, perfect linear Eyring plots were obtained, and this allowed us to calculate the activation enthalpy (ΔH^*) and entropy (ΔS^*). In the related prolyl oligopeptidase, several water molecules form an extended hydrogen bond system in and around the oxyanion hole (V. Fülöp, University of Warwick, Coventry, U.K., personal communication). The hydration zone around the active site may increase both the ΔH^* and ΔS^* values of the reaction if the ordered water molecules are released into the bulk water upon substrate binding. Therefore, ΔH^* and ΔS^* for substrate RR have been examined with both the wild type and the Tyr452Phe variant, which presumably holds a less stable water structure at the oxyanion binding site. It is seen in Table 7 that ΔS^* is positive in all cases, which may be a consequence of the release of ordered water molecules into the bulk solvent. Otherwise, ΔS^* would be negative because the transition state is usually more ordered than the ground

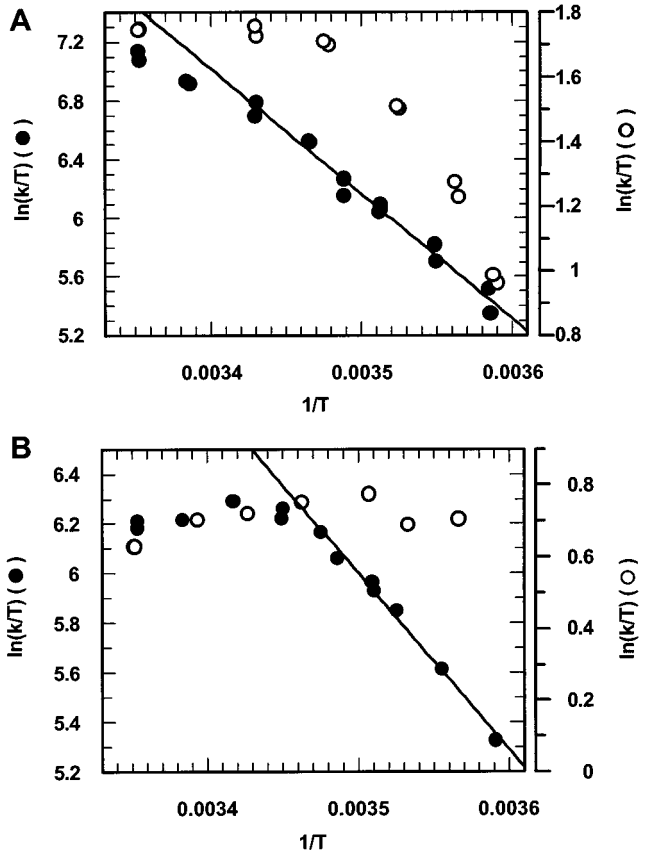

FIGURE 7: Eyring plots for the reactions of oligopeptidase B (●) and its Tyr452Phe variant (○) in the presence of 1 M NaCl. (A) The reactions of substrate CR were assessed with 10−42 nM wild-type enzyme and 0.6−2.6 μM Tyr452Phe. (B) The reactions of substrate RC were assessed with 37−50 nM wild-type enzyme and 0.5−1.6 μM Tyr452Phe. The thermodynamic parameters obtained from the linear region are shown in Table 7.

state of the reaction. Removal of the tyrosine OH group increases ΔH^* because in the absence of hydrogen bond formation the transition state becomes less stabilized. In contrast, ΔS^* becomes less positive because the transition state is less ordered without the stabilization by Tyr452. Interestingly, upon removal of the OH group of Tyr452, the change in the $T\Delta S^*$ term of ΔG^* is significantly higher than in ΔH^*. This contrasts with the generally accepted anticipation that the oxyanion binding site would only function as an electrophilic catalyst, which should be manifested in ΔH^* rather than in ΔS^*. However, in the absence of the "iceberg" (water molecules firmly bound to the enzyme or substrate), fewer water molecules are removed on going to the transition state, so the major alteration occurs in ΔS^*.

The activation parameters for the reactions of the Tyr452Phe variant with substrates CR and RC could not be determined, as linear Eyring plots were not obtained (Figure 7). The curve declined even at low temperatures (substrate CR), or was practically independent of the temperature (substrate RC), whereas in the reaction of the wild-type enzyme, an acceptable straight line was found with both substrates. For the wild-type enzyme, the difference between the reactions of the two substrates is also evident from the ΔH^* and ΔS^* values (Table 7). The reaction of the enzyme variant with substrate RC is almost independent of temperature (Figure 7B), suggesting that the catalysis is an entropy-driven process

even in the low-temperature range, whereas with the wild-type enzyme, the predominant $T\Delta S^*$ term of ΔG^* is only shown above 25 °C. This underlines the importance of the OH group of Tyr452 as both a binding entity and an electrophilic catalyst.

Conclusion. Oligopeptidase B has two carboxyl dyads, which account for the binding of a pair of basic residues. One of these carboxyl groups has a pK_a of ~6.5, whose ionization and that of the catalytic imidazole group overlap, and this perturbs the acid limb of the bell-shaped pH−rate profile. The pK_a values of the histidine and carboxyl groups are clearly separated by titration with a product-like inhibitor. The dyad carboxyl groups are also involved in substrate inhibition. The NH group of the scissile peptide bond is a further constituent in substrate binding, but its interaction with the enzyme breaks down with increasing temperature. This results in an unusually low temperature optimum, providing a normal Eyring plot only in the low-temperature range. In the absence of the tyrosine OH group of the oxyanion binding site, the data do not form a linear Eyring plot at any temperature, and the reaction becomes an entropy-driven process. The NH group of the scissile peptide bond is also important in the elimination of the assumed nonproductive binding. In short, the kinetic and thermodynamic data of this work indicate that the oxyanion binding site is not just an electrophilic catalyst and the carboxyl dyads are not just substrate binding sites, but each individual group plays a multifunctional role, not recognized so far.

ACKNOWLEDGMENT

Thanks are due to Dr. V. Fülöp and Dr. G. Keserü (ELTE University, Budapest, Hungary) for helpful discussions. We are grateful to Prof. N. Andrews and Dr. R. Morty for the information about their mutagenesis studies prior to publication. The excellent technical assistance of Ms. I. Szamosi is greatly acknowledged.

REFERENCES

1. Rawlings, N. D., Polgár, L., and Barrett, A. J. (1991) *Biochem. J. 279*, 907−908.
2. Polgár, L. (1994) *Methods Enzymol. 244*, 188−200.
3. Polgár, L. (1992) *FEBS Lett. 131*, 281−284.
4. Fülöp, V., Böcskei, Z., and Polgár, L. (1998) *Cell 94*, 161−170.
5. Fülöp, V., Szeltner, Z., and Polgár, L. (2000) *EMBO Rep. 1*, 277−281.
6. Kanatani, A., Masuda, T., Shimoda, T., Misoka, F., Xu, L.-S., Yoshimoto, T., and Tsuru, D. (1991) *J. Biochem. 110*, 315−320.
7. Barrett, A. J., and Rawlings, N. D. (1992) *Biol. Chem. Hoppe-Seyler 373*, 553−560.
8. Tsuru, D., and Yoshimoto, T. (1994) *Methods Enzymol. 244*, 201−215.
9. Cazzulo, J. J. (1999) Chagas Disease, in *Proteases of Infectious Agents* (Dunn, B. M., Ed.) pp 189−203, Academic Press, London.
10. Morty, R. E., Troeberg, L., Pike, R. N., Jones, R., Nickel, P., Lonsdale-Eccles, J. D., and Coetzer, T. H. T. (1998) *FEBS Lett. 433*, 251−256.
11. Morty, R. E., Lonsdale-Eccles, J. D., Morehead, J., Caler, E. V., Mentele, R., Auerswald, E. A., Coetzer, T. H., Andrews, N. W., and Burleigh, B. A. (1999) *J. Biol. Chem. 274*, 26149−26156.
12. Morty, R. E., Troeberg, L., Powers, J. C., Ono, S., Lonsdale-Eccles, J. D., and Coetzer, T. H. (2000) *Biochem. Pharmacol. 15*, 1497−1504.
13. Burleigh, B. A., Caler, E. V., Webster, P., and Andrews, N. W. (1997) *J. Cell Biol. 136*, 609−620.
14. Caler, E. V., de Avalos, S. V., Haynes, P. A., Andrews, N. W., and Burleigh, B. A. (1998) *EMBO J. 17*, 4975−4986.
15. Caler, E. V., Morty, R. E., Burleigh, B. A., and Andrews, N. W. (2000) *Infect. Immun. 68*, 6602−6610.
16. Morty, R. E., Londsdale-Eccles, J. D., Mentele, R., Auerswald, E. A., and Coetzer, T. H. (2001) *Infect. Immun. 68*, 27757−27761.
17. Ashall, F., Harris, D., Roberts, H., Healy, N., and Shaw, E. (1990) *Biochim. Biophys. Acta 1035*, 293−299.
18. Kornblatt, M. J., Mpimbaza, G. W. N., and Lonsdale-Eccles, J. D. (1992) *Arch. Biochem. Biophys. 293*, 25−31.
19. Polgár, L. (1997) *Proteins: Struct., Funct., Genet. 28*, 375−379.
20. Polgár, L. (1989) *Mechanisms of Protease Action*, pp 87−122, CRC Press, Boca Raton, FL.
21. Bryan, P., Pantoliano, M. W., Quill, S. G., Hsiao, H.-Y., and Poulos, T. (1986) *Proc. Natl. Acad. Sci. U.S.A. 83*, 1743−1745.
22. Carter, P., and Wells, J. A. (1990) *Proteins: Struct., Funct., Genet. 7*, 335−342.
23. Szeltner, Z., Renner, V., and Polgár, L. (2000) *Protein Sci. 9*, 353−360.
24. Polgár, L., and Felföldi, F. (1998) *Proteins: Struct., Funct., Genet. 30*, 424−434.
25. Ellis, K. J., and Morrison, J. F. (1982) *Methods Enyzmol. 87*, 404−426.
26. Leatherbarrow, R. J. (1998) *GraFit*, version 4, Erithacus Software Ltd., Staines, U.K.
27. Polgár, L. (1999) *Biochemistry 38*, 15548−15555.
28. Gérczei, T., Keserü, G. M., and Náray-Szabó, G. (2000) *J. Mol. Graphics Modell. 18*, 7−17.
29. Siezen, R. J., Creemers, J. W. M., and Van de Ven, W. J. M. (1994) *Eur. J. Biochem. 222*, 255−266.
30. Asbóth, B., and Polgár, L. (1983) *Biochemistry 22*, 117−122.
31. Russel, A. J., and Fersht, A. R. (1987) *Nature 328*, 496−500.
32. Cornish-Bowden, A. (1995) *Fundamentals of Enzyme Kinetics*, pp 118−121, Portland Press Ltd., London.
33. Fülöp, V., Szeltner, Z., Renner, V., and Polgár, L. (2001) *J. Biol. Chem. 276*, 1262−1266.
34. Ayala, Y. M., and Di Cera, E. (2000) *Protein Sci. 9*, 1589−1593.

BI016016Z